

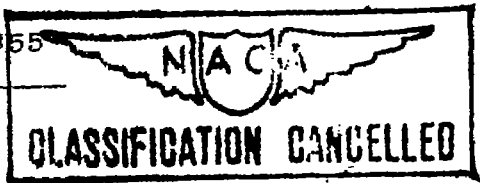
Contains classified information affecting  
interests of the United States within  
the Espionage Act, U.S. 20:1 and  
Section 7 of the War Information Act.  
The transmission or the revelation of its contents  
to an unauthorized person is prohibited by  
law. Classification may be imparted only  
to the military and naval Services of the  
United States, appropriate civilian officers and employees  
of the Federal Government who have a legitimate interest  
therein, and to United States citizens of known loyalty and  
discretion who of necessity must be informed thereof.

RECORDED  
11 1942

TECHNICAL NOTES

NATIONAL ADVISORY COMMITTEE FOR AERONAUTICS

No. 855



A METHOD FOR DETERMINING THE CAMBER AND TWIST OF A  
SURFACE TO SUPPORT A GIVEN DISTRIBUTION OF LIFT

By Doris Cohen

Langley Memorial Aeronautical Laboratory  
Langley Field, Va.

Washington  
August 1942

REF ID: A62712  
RESTRICTED

E R R A T A

NATIONAL ADVISORY COMMITTEE FOR AERONAUTICS

TECHNICAL NOTE NO. 855

A METHOD FOR DETERMINING THE CAMBER AND TWIST OF A  
SURFACE TO SUPPORT A GIVEN DISTRIBUTION OF LIFT

Page 8, line 17: Change  $\Gamma$  to  $\bar{\Gamma}$ .

Figure 5: Change subscript  $2n$  to  $2N$ .

Figure 6: Remove bar on  $\bar{\Gamma}$ .

## NATIONAL ADVISORY COMMITTEE FOR AERONAUTICS

## TECHNICAL NOTE NO. 855

A METHOD FOR DETERMINING THE CAMBER AND TWIST OF A  
SURFACE TO SUPPORT A GIVEN DISTRIBUTION OF LIFT

By Doris Cohen

## SUMMARY

A graphical method is described for finding the shape (camber and twist) of an airfoil having an arbitrary distribution of lift. The method consists in replacing the lifting surface and its wake with an equivalent arrangement of vortices and in finding the associated vertical velocities.

By a division of the vortex pattern into circular strips concentric about the downwash point instead of into the usual rectangular strips, the lifting surface is reduced for each downwash point to an equivalent loaded line for which the induced velocity is readily computed. The ratio of the vertical velocity to the stream velocity is the slope of the surface in the free-stream direction.

As an illustration, the shape of the wing consistent with the pressure distribution derived from the two-dimensional theories is found for two wings: a straight elliptical wing and one with 30° sweepback.

Application of the method to solve the reverse problem - finding the lift distribution over a given surface - is briefly discussed.

## INTRODUCTION

Because of the effect that the pressure gradients over the surface of a wing have on the drag, it would be of considerable advantage to be able to specify the camber and the twist of a wing that would produce a desired distribution of lift. Present methods of airfoil design depend on two-dimensional-flow theories, which treat the spanwise and chordwise components of the flow independently.

Although a theoretical treatment of three-dimensional flow is given by Prandtl (reference 1) and calculations have been made for special cases (references 2 and 3), no practical procedure for the arbitrary lifting surface is indicated.

In the present paper, a method is described whereby the camber and the twist of a surface of arbitrary plan form may be determined so as to support a specified distribution of lift. For this method, the lifting surface and its wake are replaced by a distribution of vortices in a plane. The vertical velocity induced at any point on the surface by the vortex system defines the slope of the surface at that point. Thus, the problem becomes the determination of the induced velocities. A method is presented for determining these velocities which, by employing chiefly graphical means, eliminates the difficult integrations that have limited previous work.

The substitution of a plane vortex sheet for the lifting surface is analogous to the standard procedure of the two-dimensional thin wing-section theory (see, for example, reference 4, p. 87), in which the flow about a thin, cambered section is approximated by an arrangement of vortices along the chord line. Inasmuch as the induced normal velocities are assumed to be substantially the same at the chord line and at the airfoil, the ratio of these velocities to the free-stream velocity gives the slope of the camber line. In three-dimensional flow a reference plane is assumed, so situated that the airfoil may be considered to be a slight deviation from it. Upon this plane the plan form and the pressure distribution of the surface are projected. As in two-dimensional treatments, the slope is calculated in the free-stream direction.

The substitution of a vortex sheet for a lifting surface is discussed at some length by von Kármán (reference 5, p. 15). In the application of the method, however, the vortices are generally assumed to have a rectilinear distribution. Even with this limitation, the evaluation of the integrals involved in finding the induced velocities presents considerable difficulty. (See ch. IV, sec. 15, of reference 5, where the formulas are developed for a rectangular wing.) The integration is greatly simplified by the introduction of polar coordinates so chosen that the elements of integration are circular strips concentric about the point at which the downwash is to be found. Application of this method is not restricted to any particu-

lar arrangement of vortices or to any specific form of the surface.

Although the procedure described is for the determination of the surface that will fit a required pressure distribution, it may also be adapted to effect the reverse analysis, that is, to find the pressure distribution over an arbitrary surface. When the surfaces that fit several assumed pressure distributions have been found, the required surface can be built up by a linear combination of these solutions. If a reasonably close distribution can be assumed as a first approximation, finding the surface to fit the assumed distribution will indicate the manner in which that distribution must be corrected to fit the given surface.

#### DETERMINATION OF THE VORTEX PATTERN FROM THE PRESSURE DISTRIBUTION

The vortex pattern is obtained by integrating the chordwise pressure distribution back from the leading edge at several stations along the span. The circulation or vortex strength  $\Gamma$  will be shown to be proportional to this integral; the lines connecting the points where the values of the integral are equal therefore define the vortex lines.

In figure 1, a distribution of lift is arbitrarily specified for a tapered wing in straight flight. The corresponding vortex lines are drawn on the plan form of the wing and in the wake in figure 2 to show a typical vortex pattern.

The demonstration of the relation between the pressure distribution and the vortex pattern is given in the following paragraphs.

In the replacement of a lifting surface by a vortex sheet, the assumption is made that the pressure increments due to the presence of the airfoil in the stream are equal and opposite on the upper and lower surfaces, as would be true in the case of a thin plate at a small angle of attack. The substitution is still admissible in the calculation of lift when the thickness is not negligible, because the difference between the velocities on the upper and lower surfaces at any position and not the magnitude of each increment determines the lift at that point.

Thus, let  $\Delta V_u$  and  $\Delta V_l$  represent for any point the local velocity increments on the upper and the lower surfaces due to the plate or to the vortices that are equivalent to it; let  $u_u$  and  $u_l$  be the magnitude of their components in the direction of the free-stream velocity  $\underline{V}$ ; let  $v_u$  and  $v_l$  be the components normal to  $\underline{V}$  in the plane of the wing; and let  $w_u$  and  $w_l$  be the components normal to the wing. Then, the pressure on the surfaces would be

$$\begin{aligned} p_u &= \frac{1}{2} \rho \left| \underline{V} + \Delta V_u \right|^2 \\ &= \frac{1}{2} \rho \left[ (V + u_u)^2 + v_u^2 + w_u^2 \right] \\ &= \frac{1}{2} \rho (V^2 + 2Vu_u + u_u^2 + v_u^2 + w_u^2) \\ &= \frac{1}{2} \rho (V^2 + 2Vu_u) \end{aligned}$$

neglecting second-order effects; and, similarly,

$$p_l = \frac{1}{2} \rho (V^2 + 2Vu_l)$$

The resulting lift per unit area is then the difference in pressure, or

$$\Delta p = \frac{1}{2} \rho 2V (u_u - u_l) \quad (1)$$

The derivation of the equivalent vortex pattern follows directly from equation (1). If  $ds\Gamma$  represents the element of circulation around a small length  $ds$ , parallel to  $\underline{V}$ , over which the velocities  $u_u$  and  $u_l$  may be considered constant, the following relation holds:

$$ds\Gamma = (u_u - u_l) ds \quad (2)$$

from which equation (1) may be rewritten

$$\Delta p = \rho V \frac{\partial \Gamma}{\partial s} \quad (3)$$

Thus, the lift at every point is proportional to  $\frac{\partial \Gamma}{\partial s}$ , or the cross-stream component of the vorticity. Consider now a narrow strip of varying width just behind the leading edge of the vortex sheet, such that  $\int \Delta p \, ds$  is constant along the strip. Such a strip would represent a vortex element of strength  $\int \Delta p \, ds$ . A second vortex element could be defined in the same way to lie just behind the first. From equation (3), however,

$$\frac{1}{\rho V} \int \Delta p \, ds = \Gamma \quad (4)$$

Equation (4) defines the function  $\Gamma$  for any point on the lifting surface as the total circulation ahead of the point.\* Thus, the boundaries of the vortex element are lines of equal  $\Gamma$ .

If the vortex elements are reduced in size and increased in number to form a continuous vortex sheet, their pattern is indicated, as in figure 1, by the contour lines of the function  $\Gamma$ . In order to satisfy the Kutta condition that there be no pressure difference across the trailing edge, these lines must leave the wing parallel to the stream velocity, as shown by equation (3). They then follow the streamlines down the wake. The drawing of these contour lines from the integral of the pressure distribution is the first step of the procedure for finding the camber and the twist of the lifting surface.

#### DETERMINATION OF THE INDUCED VERTICAL VELOCITIES

The induced vertical velocity at any point of the plane is obtained by integrating the Biot-Savart equation

---

\*The function  $\Gamma$  is numerically equal to the difference in velocity potential between the surfaces, for, at any point,  $u_u = \partial \phi_u / \partial s$  and  $u_l = \partial \phi_l / \partial s$ , where  $\phi_u$  and  $\phi_l$  are the potential functions over the upper and lower surfaces of the airfoil, respectively. From equation (2),

$$\frac{\partial \Gamma}{\partial s} = \frac{\partial \phi_u}{\partial s} - \frac{\partial \phi_l}{\partial s}$$

or

$$\Gamma = \phi_u - \phi_l$$

over the entire vortex pattern just described. The resulting double integration is reduced to a single integral by a relatively simple graphical procedure if a system of polar coordinates having its origin at the point is employed.

Let it be required to find the downwash  $w$  at a point  $P$  of the vortex pattern just described. Consider a small sector of the plane included between two radii from  $P$ , the angle between the radii being  $d\psi$  (fig. 3). At any distance  $r$  from  $P$ , the radii will cut off a small length  $dl$  of a certain vortex element. If the width of the element in the radial direction is  $dr$ , the strength of the vortex element is  $-\frac{\partial \Gamma}{\partial r} dr$ . Then, by Biot-Savart's rule, the downwash at  $P$  due to the small length of vortex will be

$$dw = -\frac{1}{4\pi} \frac{1}{r^2} \frac{\partial \Gamma}{\partial r} dr dl \sin \beta \quad (5)$$

where  $\beta$  is the angle between the vortex element and the radius. The length  $dl \sin \beta$  is the projection of  $dl$  on the circumference of the circle of radius  $r$  around  $P$ , so that

$$dl \sin \beta = rd\psi$$

and

$$dw = -\frac{1}{4\pi r} \frac{\partial \Gamma}{\partial r} dr d\psi \quad (6)$$

The total downwash at  $P$  would be obtained by integrating (6) over  $0 \leq r \rightarrow \infty$  and through  $360^\circ$  of  $\psi$ . Thus,

$$w = \int_0^\infty \int_0^{2\pi} -\frac{1}{4\pi r} \frac{\partial \Gamma}{\partial r} d\psi dr \quad (7)$$

In order to evaluate the double integral of equation (7), the relation (Liebniz's rule)

$$\int_0^{2\pi} \frac{\partial \Gamma}{\partial r} d\psi = \frac{d}{dr} \int_0^{2\pi} \Gamma d\psi \quad (8)$$

is used to reduce the first integration to a graphical procedure.

The first step in evaluating  $w$  is to draw on the vortex pattern circles of various radii about  $P$ . Around any one circle (see fig. 4) the function  $\Gamma$  will take on values indicated by the intersections of the circle with the contour lines of  $\Gamma$ . If these values of  $\Gamma$  are plotted against the angle  $\psi$  - measured, let us say, from the free-stream direction - graphical integration will give  $\int_0^{2\pi} \Gamma d\psi$  for each circle. It is somewhat more convenient to plot  $\Gamma$  against  $\psi/2\pi$ . Then the integral will be the average value of  $\Gamma$  around the circle, designated in the usual way by

$$\bar{\Gamma} = \int_0^{2\pi} \frac{\Gamma}{2\pi} d\psi \quad (9)$$

Then  $\bar{\Gamma}$  is a function of  $r$ . (See fig. 5.) From equation (8),

$$\int_0^{2\pi} \frac{\partial \Gamma}{\partial r} d\psi = 2\pi \frac{d\bar{\Gamma}}{dr} \quad (10)$$

so that

$$w = - \int_0^{\infty} \frac{1}{2r} \frac{d\bar{\Gamma}}{dr} dr \quad (11)$$

For the evaluation of equation (11), first plot  $\bar{\Gamma}$  against  $r$ , as in figure 5. The curve will approach an asymptote, which is readily found from the expression for the load curve across the wake. Thus, when  $r$  is large,  $d\psi = \frac{dy}{r}$  and equation (9) reduces to

$$\bar{\Gamma} = \frac{1}{r} \int_{-b/2}^{b/2} \Gamma(y) dy \quad (12)$$

where  $b/2$  is the semispan of the wing. If the area under the load curve across the wake is  $A$ , then for very large values of  $r$

$$\bar{\Gamma} = \frac{A}{2\pi r} \quad (13)$$

The plot of  $\bar{\Gamma}(r)$  should be carried out to a value of  $r$  such that the curve approaches this asymptote within the accuracy of the work.

The load curve of figure 5 is a typical one. The following method has been found particularly suited to the determination of the downwash at the origin of such a curve. The first section of the curve (designated by I), starting with zero slope, is approximated up to the inflection point, or to a point  $r_0$  somewhat ahead of it, by an expression of the form  $\bar{\Gamma} = a_0 - a_2 r^2 - a_4 r^4$ . Additional terms might be used but are generally not necessary. The downwash due to a curve of the general form  $\bar{\Gamma} = a_0 - a_n r^n$ , ( $n > 1$ ), at  $r = 0$  is given by

$w = - \frac{a_n}{2} \frac{n}{n-1} (r_B^{n-1} - r_A^{n-1})$ , where  $r_A$  and  $r_B$  are the end values of  $r$  for the interval over which the curve extends. The downwash contributed by the first section of the load  $\bar{\Gamma} = a_0 - a_2 r^2 - a_4 r^4$  is therefore

$$w(I) = \frac{1}{2} \left( 2a_2 r_0 + \frac{4}{3} a_4 r_0^3 \right) \quad (14)$$

The part of the curve immediately following  $r = r_0$  has a critical effect on the value of the downwash, at the same time being usually too irregular to be approximated for any distance by a simple algebraic expression. It is therefore advisable to proceed as in numerical integration, dividing the curve into a finite number of small sections and considering each section of the curve to have a simple mathematical expression. Because the effectiveness of the variation of load depends on its closeness to the downwash point, the intervals are taken in geometric rather than arithmetic progression. Thus, the abscissas are  $r_0, kr_0, k^2 r_0, \dots$  etc., where the ratio  $k$  is a number, usually between 1 and 2, determined by the size of the intervals required for accurate representation of the curve immediately following  $r_0$ . The usual procedure now would be to assume the curve to be a straight line over each small interval but when the curvature is largely in one direction, as it is in these curves, this assumption introduces a small but cumulative error, which may amount to 10 percent or more in the total. The following method, which fits the curve with a succession of parabolae, is found to give very good accuracy with no increase in computation. The method is best presented in tabular form:

$(r_{2n} = k^{an} r_0, r_{2n+1} = k^{an+1} r_0)$			(Compute)	
$n$	$r_{2n} \ r_{2n+1}$	$\bar{\Gamma}$	$\Delta\bar{\Gamma}_{2n}$	$\Delta\bar{\Gamma}_{2n+1}$
0	$r_0$	$\bar{\Gamma}_0$	$\bar{\Gamma}_1 - \bar{\Gamma}_0$	$\frac{\Delta\bar{\Gamma}_0}{r_0}$
1	$r_1$	$\bar{\Gamma}_1$	$\bar{\Gamma}_2 - \bar{\Gamma}_1$	$\frac{\Delta\bar{\Gamma}_1}{r_0}$
2	$r_2$	$\bar{\Gamma}_2$	$\bar{\Gamma}_3 - \bar{\Gamma}_2$	$\frac{\Delta\bar{\Gamma}_2}{r_2}$
3	$r_3$	$\bar{\Gamma}_3$	$\bar{\Gamma}_4 - \bar{\Gamma}_3$	$\frac{\Delta\bar{\Gamma}_3}{r_2}$
4	$r_4$	$\bar{\Gamma}_4$	$\bar{\Gamma}_5 - \bar{\Gamma}_4$	$\frac{\Delta\bar{\Gamma}_4}{r_4}$
5	$r_5$	$\bar{\Gamma}_5$	$\bar{\Gamma}_6 - \bar{\Gamma}_5$	$\frac{\Delta\bar{\Gamma}_5}{r_4}$
6	$r_6$	$\bar{\Gamma}_6$		
$N-1$	$r_{2N-1}$	$\bar{\Gamma}_{2N-1}$	$\bar{\Gamma}_{2N-1} - \bar{\Gamma}_{2N-2}$	$\frac{\Delta\bar{\Gamma}_{2N-2}}{r_{2N-2}}$
	$r_{2N}$	$\bar{\Gamma}_{2N}$	$\bar{\Gamma}_{2N} - \bar{\Gamma}_{2N-1}$	$\frac{\Delta\bar{\Gamma}_{2N-1}}{r_{2N-2}}$

$$K_0 = k \left( k - \frac{\log k}{k-1} - 1 \right)$$

Totals:

$$\sum_{n=0}^{N-1} \frac{\Delta\bar{\Gamma}_{2n}}{r_{2n}} \quad \sum_{n=0}^{N-1} \frac{\Delta\bar{\Gamma}_{2n+1}}{r_{2n}}$$

$$K_1 = 1 - \frac{\log k}{k-1}$$

$$w = \frac{-1}{k(k-1)} \left( K_0 \sum \frac{\Delta\bar{\Gamma}_{2n}}{r_{2n}} + K_1 \sum \frac{\Delta\bar{\Gamma}_{2n+1}}{r_{2n}} \right)$$

In the following table are given the constants  $K_0$ ,  $K_1$ , and  $\frac{1}{k(k-1)}$  for several convenient values of  $k$ . Since the choice of  $k$  is not critical, the values included should serve without interpolation.

$k$	$K_0$	$K_1$	$\frac{1}{k(k-1)}$
1.02	0.01000	0.01000	49.02
1.05	.02582	.02420	19.04
1.07	.03667	.03340	13.35
1.10	.05325	.04690	9.091
1.15	.08222	.06827	5.797
1.20	.1127	.08840	4.167
1.25	.1446	.1074	3.200
1.30	.1780	.1255	2.564
1.50	.3246	.1891	1.333

The value of the ratio  $k$  that will give sufficiently small increments of  $r$  where the slope is large will probably be found to be smaller than necessary after the curve has become more regular and the distance from the origin larger. The computations may be interrupted here and the downwash  $w(II)$  contributed by the second section may be calculated. Then, using the last abscissa  $r_{2N}$  as a new starting point and a larger value of  $k$ , compute in the same way the downwash  $w(III)$  due to the remainder of the curve to a point where the difference between the curve and its asymptote is negligible.

For the portion of the curve extending to infinity (section IV of fig. 5), the previously determined asymptote is used and the downwash found analytically. Thus, from a large value  $R$  or  $r$  out to infinity,

$$w(IV) = -\frac{1}{2} \int_R^{\infty} \frac{1}{r} \cdot \frac{d\bar{F}}{dr} dr$$

from equation (10), and if  $d\bar{F}/dr$  is found from equation (13),

$$w(IV) = \frac{A_s}{8\pi R^2} \quad (15)$$

The downwash at  $P$  is then the sum  
 $w(I) + w(II) + w(III) + w(IV)$ .

It is interesting to note that the three-dimensional problem has been reduced to one of two-dimensional flow, as may be seen by replacing  $\bar{F}$  with its original expression (9) in equation (11), which may then be written

$$w(o) = \int_0^\infty \frac{d \int_0^{2\pi} \Gamma d\psi}{\frac{dr}{4\pi(r - o)}} dr \quad (16)$$

Equation (16) is recognized as the ordinary formula for the induced normal velocity with the load expressed in the form of a definite integral and suggests that the first integration (except that the factor  $1/2\pi$  was introduced) was equivalent to concentrating all the vorticity around each circle at a single point at the distance  $r$  along a line of infinite extension from  $P$ . The loaded line of figure 5 may be considered, except for the factor  $1/2\pi$ , to be the equivalent of the original lifting surface.

#### EXAMPLE

The method will be applied to check the elliptical distribution of lift conventionally assumed for an uncambered elliptical wing. This distribution, arrived at by combining the two-dimensional theories, does not take account of sweepback or stagger of the lifting elements. In the application of the present method, two cases of elliptical chord distribution will be investigated, one with a straight 50-percent-chord line, and one with the 50-percent-chord line swept back about  $30^\circ$ , the sections remaining parallel to the plane of symmetry. The calculation of the vertical velocities over the swept-back wing will be carried out herein in some detail in order to illustrate the method. The downwash will be found at several points along the three-quarter-chord line. The downwash at the three-quarter-chord point of a section is of particular interest because, from the thin wing section theory (reference 6, p. 82), the effective angle of attack of the section is given by the slope of the camber line in the neighborhood of that point, if the camber is approximately circular.

For the chordwise lift distribution, the two-dimensional flow around a flat plate as given by the thin wing section theory is assumed. This lift distribution and the circulation function obtained by integrating it are shown in figure 6. In this case the mathematical expression for the pressure difference is known and  $\Gamma$  can be found analytically. For convenience, the units have been so chosen that the maximum value of  $\Gamma$  is 1.0. If, further, all lengths are expressed in terms of the semispan (measured perpendicular to the plane of symmetry) as the unit of length, the total circulation ( $\Gamma$  at the trailing edge) is simply  $\sqrt{1 - y^2}$ , where  $y$  is the distance spanwise from the center line. The resulting contour lines of  $\Gamma$  appear, for the swept-back wing, as in figure 7. The points at which the downwash will be found are also shown.

In order to find the downwash at point B, circles spaced as shown in figure 8 are drawn about this point and the values of  $\Gamma$  indicated by the contour lines intersected by each circle are plotted against the angular location  $\psi$  of the points of intersection. Of the curves for  $\Gamma(\psi)$  corresponding to the circles of figure 8, five typical ones are shown in figure 9. The curves designated for  $r = 0.067$  and  $r = 0.20$  are characteristic of circles close to the downwash point; the curve for  $r = 0.216$  includes a point ( $\psi/2\pi = 0.883$ ) at which the circle is tangent to the leading edge of the wing; the circle of radius 0.733 lies partly ahead of the wing where  $\Gamma = 0$ , partly in the wing, and passes through the wake; the circle of radius 1.60 traverses the vortex pattern across the wake only.

The results of integrating these curves are plotted against  $r$  in figure 10. Since the circulation across the wake is  $\sqrt{1 - y^2}$ , the integral  $\Lambda$  is  $\pi/2$  and the asymptote for the curve of  $\bar{\Gamma}(r)$  is, from equation (13),  $\bar{\Gamma} = 1/4r$ . The downwash is now calculated as follows:

It is found that the polynomial

$$\bar{\Gamma} = 0.8335 - 2.70r^2 - 6.57r^4$$

fits the curve of  $\bar{\Gamma}$  through  $r = 0.20$ . Then the downwash contributed by the section from 0 to 0.2 is, from equation (14)

$$w(I) = 0.575$$

Section II, with  $k$  small, is taken to include both inflection points (there is a third inflection point at 1.78, but its effect is negligible). Table I shows the calculations for this section and for the succeeding one. Section III extends to  $r = 2.433$ , where  $\bar{\Gamma} = 0.108$  and  $1/4r = 0.103$ . The downwash induced by the asymptote from  $r = 2.433$  out to infinity is only  $1/32(2.433)^3 = 0.011$ , about 1 percent of the total due to the curve of  $\bar{\Gamma}$ , and the 5-percent error in the ordinate may therefore be neglected. The total downwash at B is then

$$w(I) + w(II) + w(III) + w(IV) = 1.156$$

The downwash at points A, C, and D is found in the same way. Figure 11 shows the curves of  $\bar{\Gamma}$  for these points. The asymptote  $\bar{\Gamma} = 1/4r$  is, of course, common to all the curves for this wing.

The downwash is plotted against the spanwise location of the points in figure 12. The quantities  $\Gamma_{\max}$  and  $b/2$ , heretofore assumed to be unity, are included to make the result nondimensional. This curve of the downwash or vertical velocity at the three-quarter-chord line, since the slope of the surface is  $w/V$ , is a measure of the amount of twist the wing must have to sustain the assumed distribution of lift. If the wing were actually flat, which was the premise in deriving the distribution from the two-dimensional theories,  $w$  would be equal to 1.0 all over the surface, so that the deviation of the curve from the line  $w = 1$  indicates the amount by which the two-dimensional theories are in error when applied to three-dimensional flow. The discontinuity in vorticity at the center line gives rise to a discontinuity in the downwash, which goes to infinity everywhere along the center section. This result indicates that the assumed condition, in which the vortex lines bend to form an angle, cannot exist in practice. The vortex lines actually would be rounded off and the load at the center reduced below that of the adjoining sections.

The corresponding curve for the straight elliptical wing is shown in figure 13. In this case, the downwash was computed also at points along the quarter-chord line. The slope of the surface was found to be less than the slope at the corresponding three-quarter-chord points. The positive camber thus indicated is very small at the center but increases sharply near the tips.

## CONCLUDING REMARKS

It is expected that the method outlined herein will be especially useful in investigating the nature of the flow near the wing tip, where two-dimensional approximations no longer can be applied. The more accurate three-dimensional treatments available are also unsuitable for this purpose because the calculations fail to converge at the tips. The method of calculation described in this paper presents no particular difficulty in these regions. As a test of the accuracy obtainable, the induced down-wash was computed at a point near the edge of a circular plate in nonlifting potential flow and was found to check almost exactly with the known solution.

Nevertheless, results obtained for the tips have qualitative rather than quantitative value (except for low angles of attack). The validity of the theory is actually limited by the existence of strong tip vortices, which may cause the vortex sheet to curl up out of the plane in which it is assumed to lie. On the other hand, the high concentration of vorticity associated with this effect adds appreciably to the drag of the wing, so that even a general indication of such a concentration of load at the tips is of value. It should be possible to design, by the use of the present method, a wing tip that would avoid this effect by providing a fairly gradual tapering off of the load spanwise. At the same time, a favorable chordwise gradient could be specified. Thus, it appears likely that an optimum tip for low drag could be deduced.

Langley Memorial Aeronautical Laboratory,  
National Advisory Committee for Aeronautics,  
Langley Field, Va., May 16, 1942.

## REFERENCES

1. Prandtl, L.: Recent Work on Airfoil Theory. T.M. No. 962, NACA, 1940.
2. Kinner, W.: Die kreisförmige Tragfläche auf potential-theoretischer Grundlage. Ing.-Archiv, VIII Bd., Heft 1, Feb. 1937, pp. 47-80.
3. Krienes, Klaus: The Elliptic Wing Based on the Potential Theory. T.M. No. 971, NACA, 1941.
4. Glauert, H.: The Elements of Aerofoil and Airscrew Theory. The Univ. Press (Cambridge), 1930.
5. von Kármán, Th., and Burgers, J. M.: General Aerodynamic Theory - Perfect Fluids. Vol. II, div. E of Aerodynamic Theory, W. F. Durand, ed., Julius Springer (Berlin), 1935.
6. Munk, Max M.: Fundamentals of Fluid Dynamics for Aircraft Designers. The Ronald Press Co., 1929.

TABLE I  
DOWNWASH COMPUTATIONS

$r$	$\Gamma$	$\Delta\Gamma$	$\frac{\Delta\Gamma_{an}}{r_{an}}$	$\frac{\Delta\Gamma_{an+1}}{r_{an}}$
Section II: $k = 1.07$				
0.200	0.715	-0.025	-0.125	
.214	.690	-.033		-0.165
.229	.657	-.021	-.092	
.245	.636	-.016		-.070
.262	.620	-.014	-.053	
.280	.606	-.013		-.050
.300	.593	-.011	-.033	
.321	.582	-.013		-.043
.344	.569	-.009	-.026	
.368	.560	-.010		-.029
.393	.550			
Totals:			-.329	-.357
$w(II) = 0.320$				
Section III: $k = 1.20$				
0.393	0.550	-0.026	-0.066	
.472	.524	-.027		-0.069
.566	.497	-.044	-.078	
.679	.453	-.074		-.131
.815	.379	-.062	-.076	
.978	.317	-.049		-.060
1.173	.268	-.049	-.042	
1.408	.219	-.066		-.056
1.790	.153	-.022	-.012	
2.028	.131	-.023		-.013
2.433	.108			
Totals:			-.274	-.329
$w(III) = 0.250$				

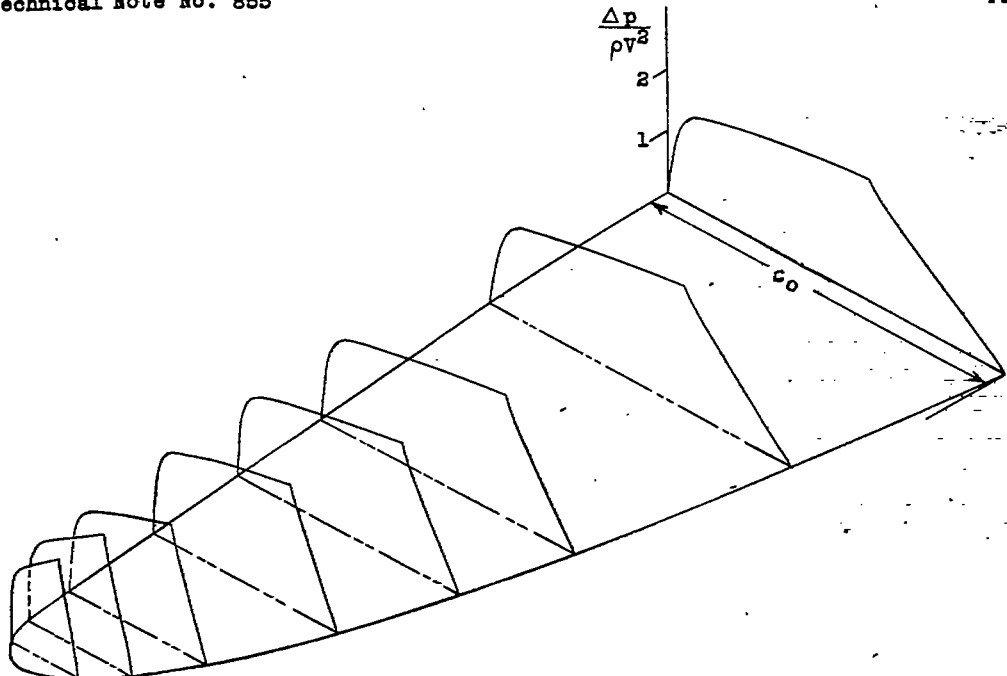


Figure 1.- An arbitrary distribution of lift assumed for a tapered wing in straight flight, from which the vortex lines of figure 2 were derived.

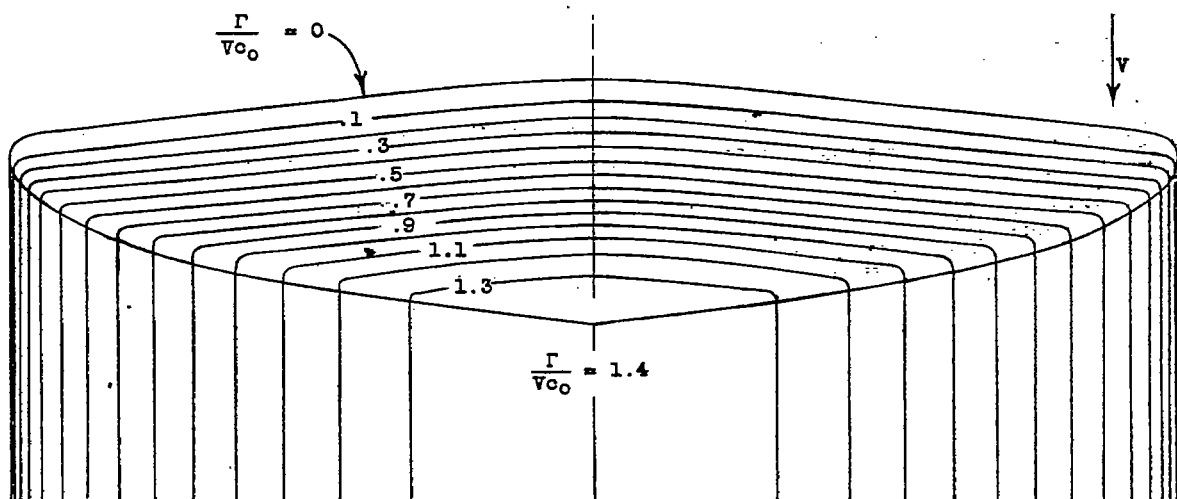


Figure 2.- Contour lines of circulation function, or vortex pattern, obtained by integrating the pressure distribution of figure 1.

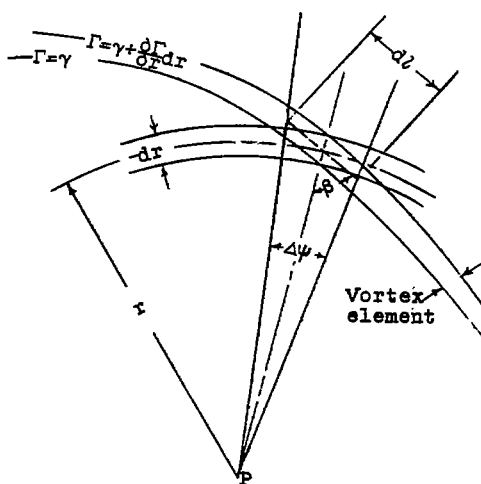


Figure 3.- Diagram for derivation of downwash formula:  $dw = \frac{1}{4\pi r} \frac{\partial \Gamma}{\partial r} dr d\Psi$ .

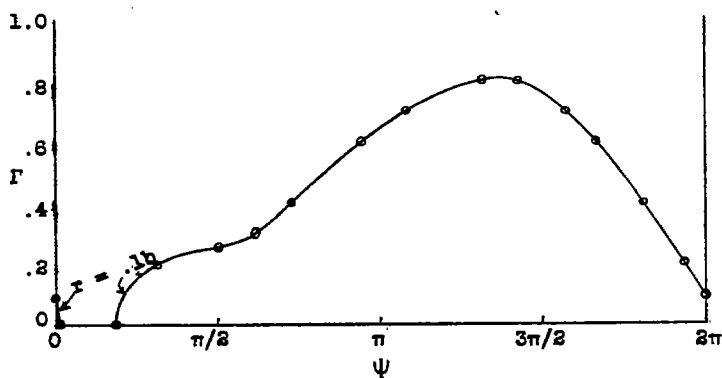
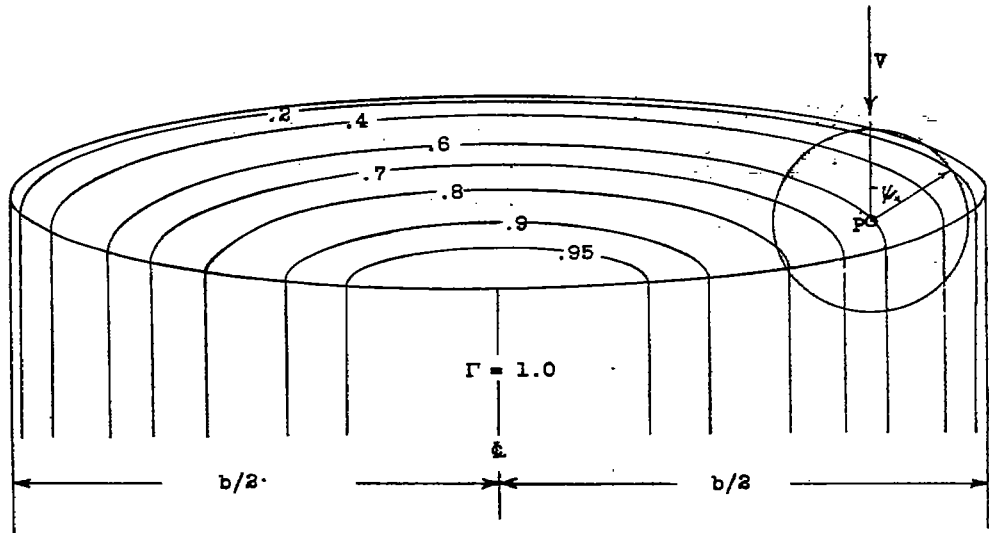


Figure 4.- Variation of  $\Gamma$  around circle, plotted against  $\Psi$  from intersections of the circle with the contour lines. Additional points at  $\Psi = 0$  and at  $\Psi = \pi/8$  are computed.

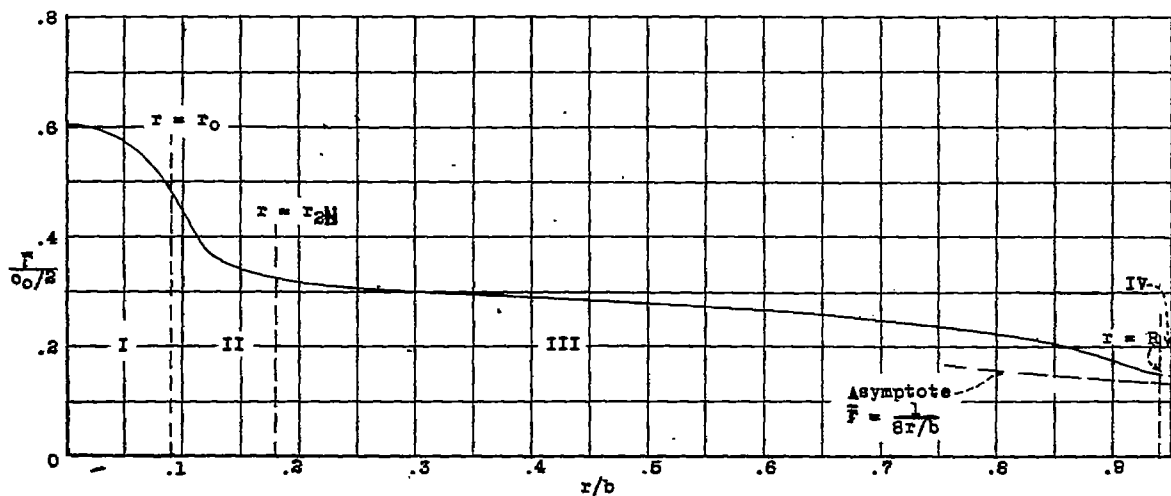
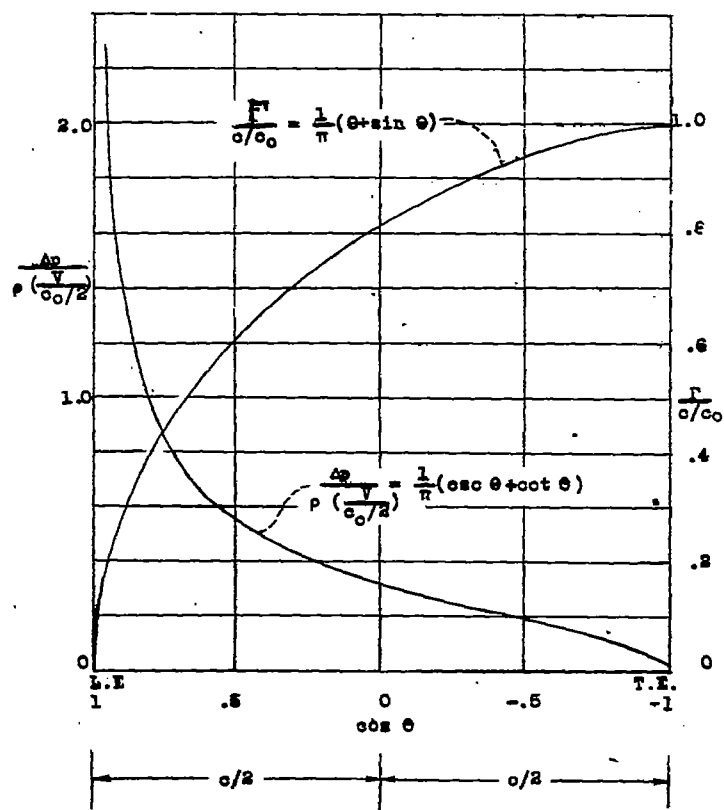
Figure 5.- Typical curve for  $F(r)$ . (Curve for point P of figure 4).

Figure 6.- Chordwise pressure distribution and circulation function assumed for figure 7 from the two-dimensional flow theory for a flat plate.

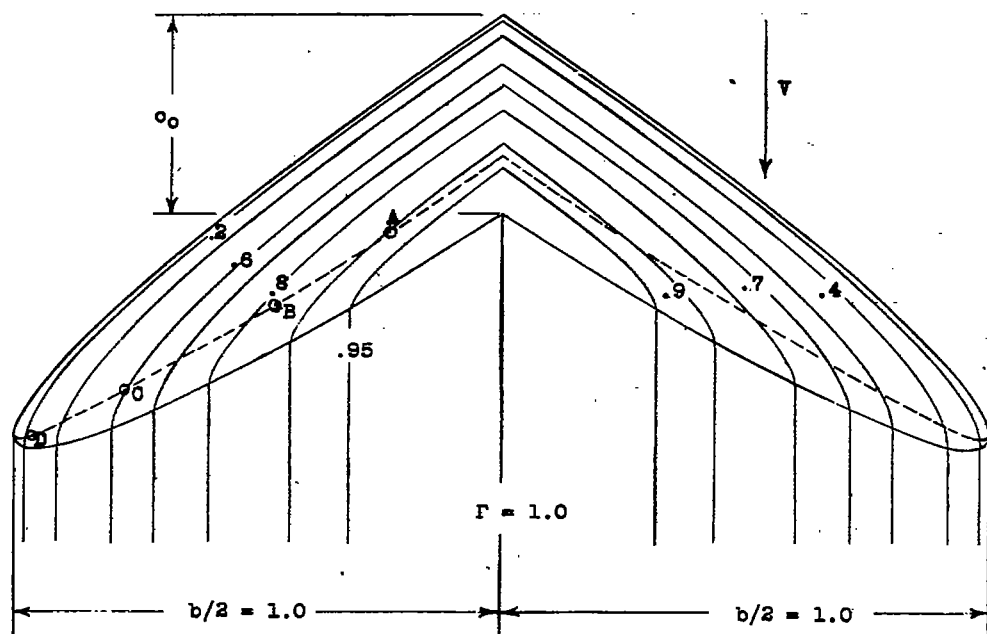


Figure 7.- Contour lines of elliptically distributed load over sweptback wing and wake.  
 $\Delta = 6.$

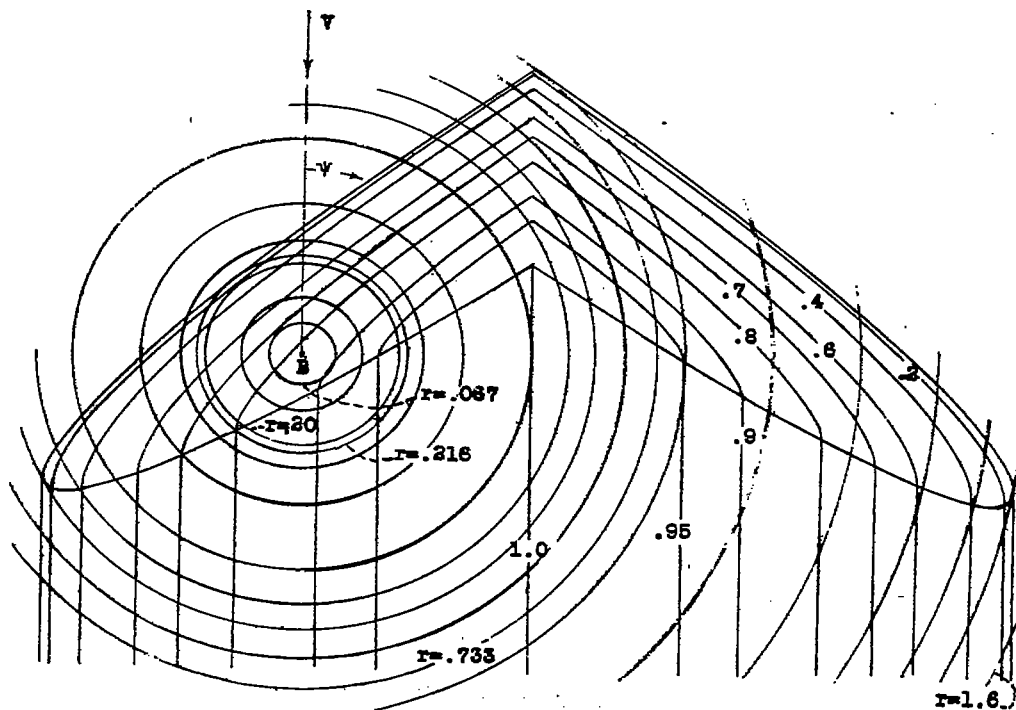


Figure 8.- Circles of integration drawn on vortex pattern. The circles corresponding to the curves of figure 9 are identified.

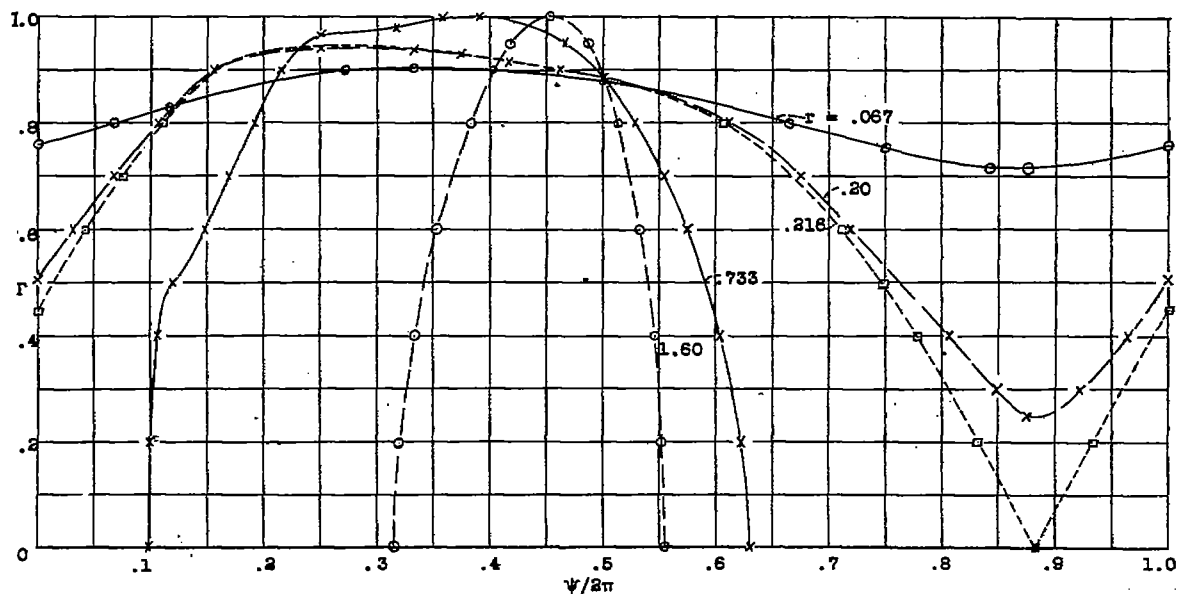


Figure 9.- Typical curves for the variation of  $F$  around a circle. The curves shown correspond to the circles identified in figure 8.

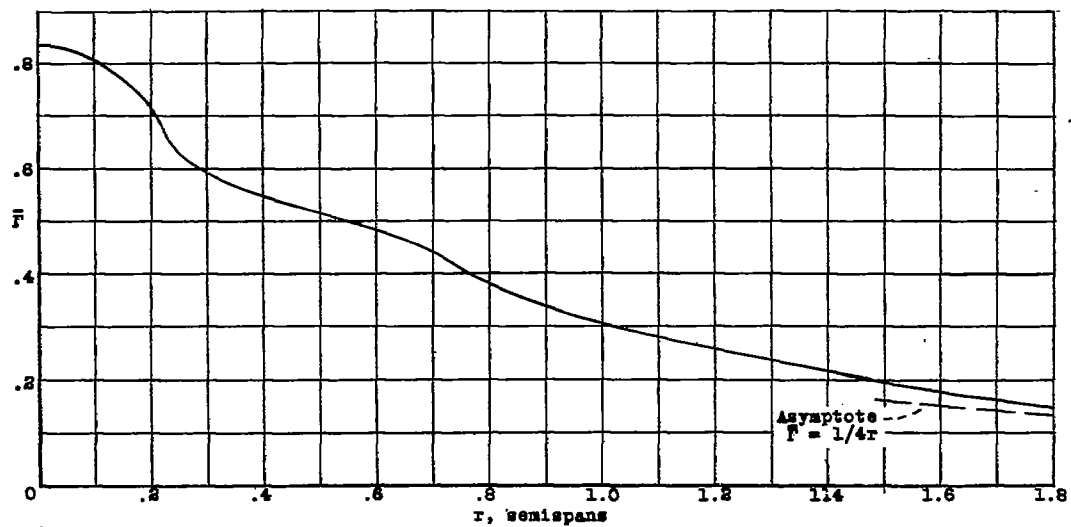


Figure 10.- Curve of  $\bar{F}(r)$  for point B of figure 7.

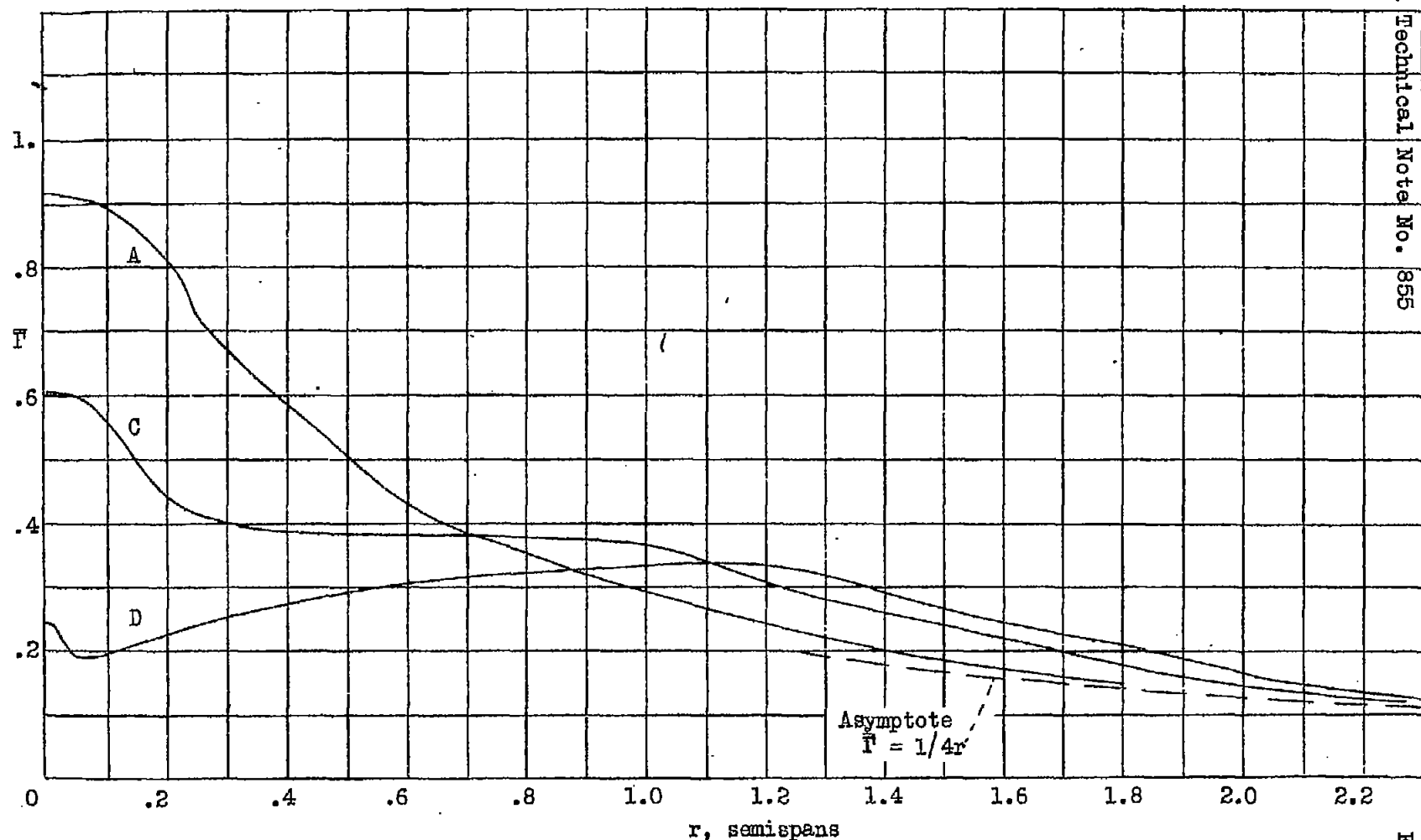


Figure 11.-- Equivalent loaded lines for points A, C, and D of the sweptback wing of Figure 8.

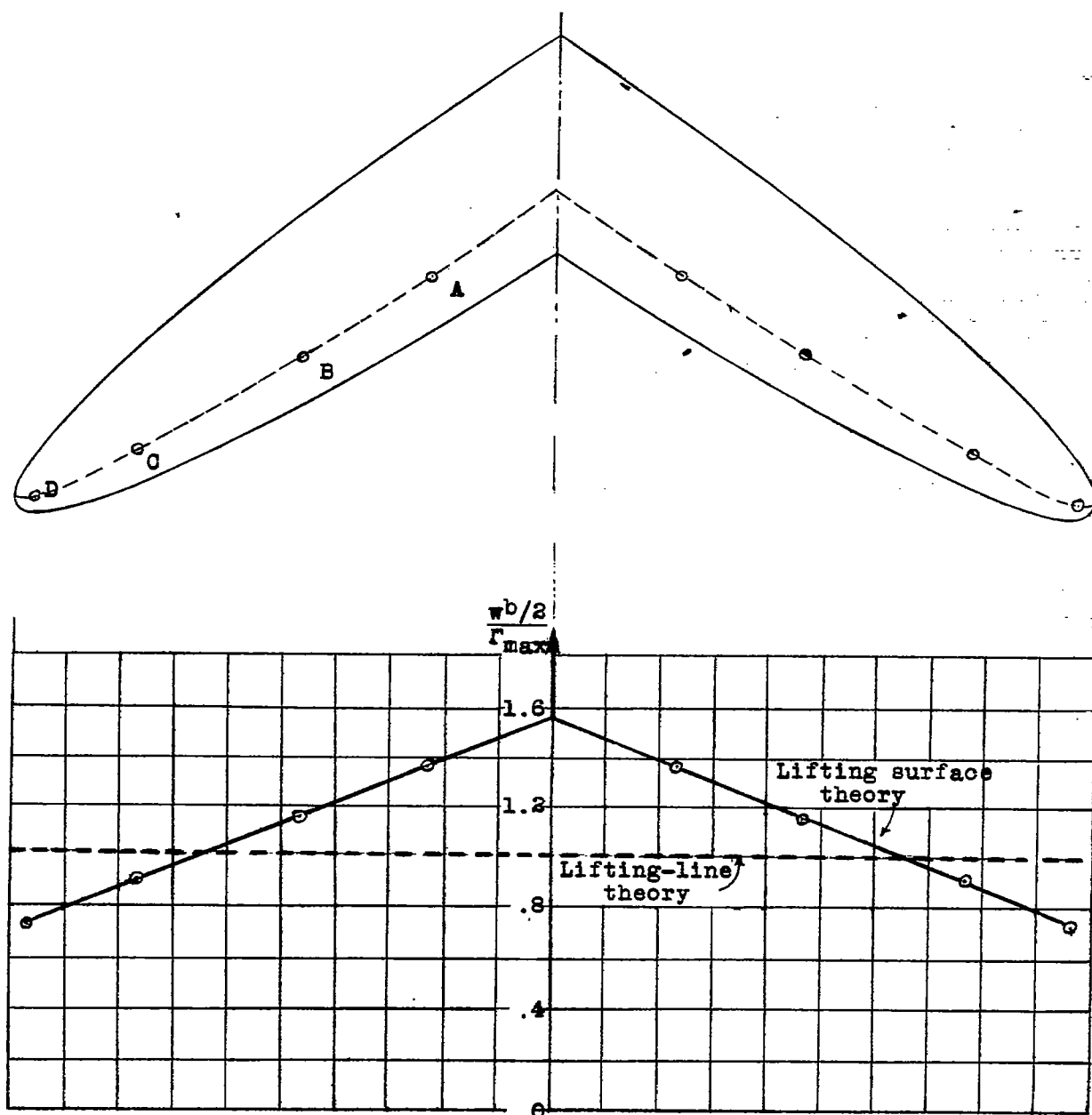


Figure 12.- Vertical velocity  $w$  at the three-quarter chord line of the swept-back wing with distribution of load calculated by two-dimensional-flow theories.

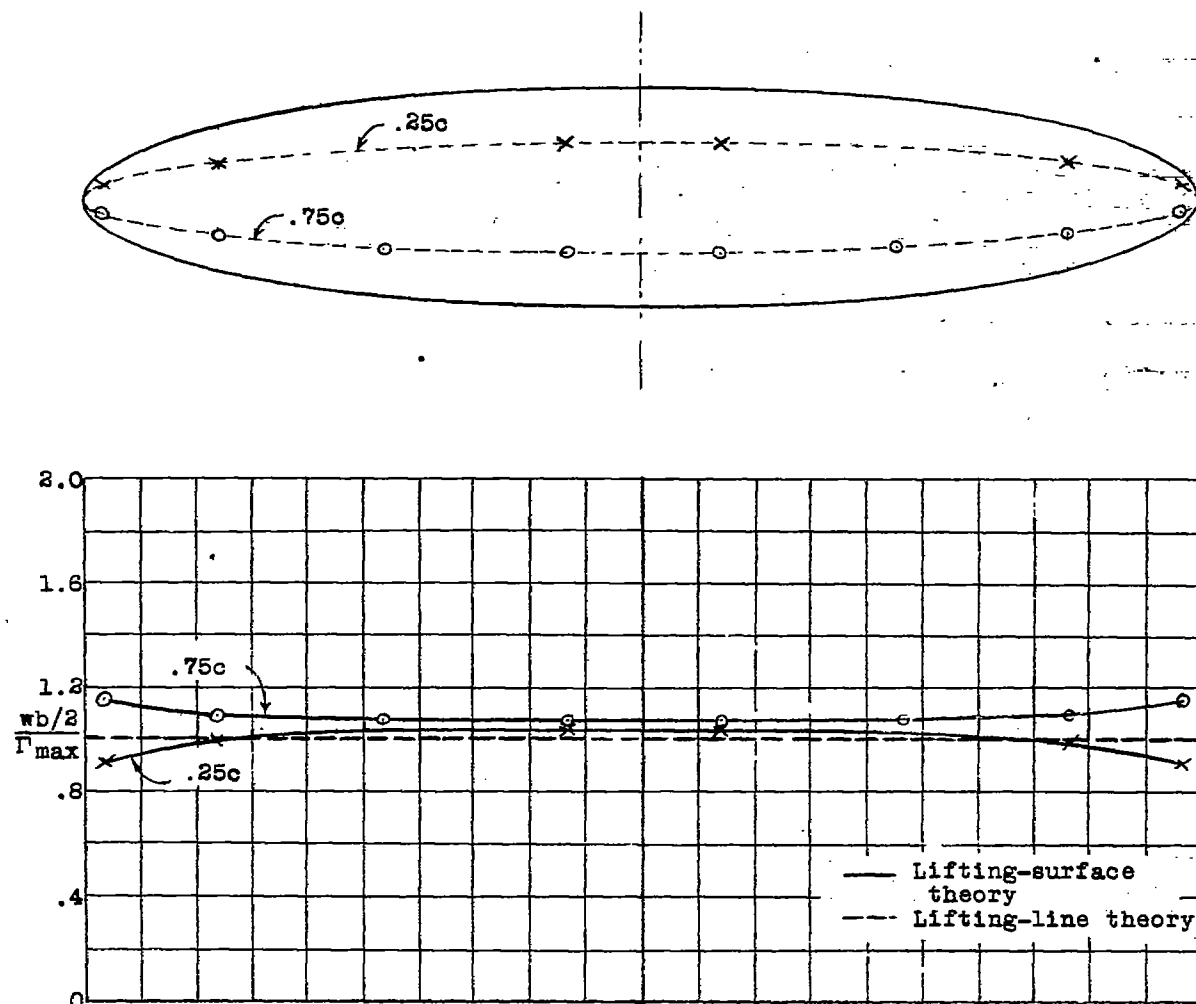


Figure 13.- Vertical velocity  $w$  at points on straight elliptical wing,  
 $A = 6$ , with distribution of load calculated by two-dimensional-flow theories.